

# Time-dependent thermal effects in GRB afterglows

K.A.Postnov<sup>a</sup>\*, S.I.Blinnikov<sup>b</sup>, D.I.Kosenko<sup>a</sup>, E.I.Sorokina<sup>a</sup>

<sup>a</sup>Sternberg Astronomical Institute, 119992 Moscow, Russia

<sup>b</sup>Institute of Theoretical and Experimental Physics, 117218 Moscow, Russia

Time-dependent thermal effects should accompany standard non-thermal afterglows of GRB when gamma-rays pass through inhomogeneous surroundings of the GRB site. Thermal relaxation of an optically thin plasma is calculated using time-dependent collisional ionization of the plasma ion species. X-ray emission lines are similar to those found in the fading X-ray afterglow of GRB 011211. Thermal relaxation of clouds or shells around the GRB site could also contribute to the varying late optical GRB afterglows, such as in GRB021004 and GRB030329.

## 1. Time-dependent X-ray emission from a thermal plasma

Determination of physical parameters of astrophysical sources with plasma densities up to  $10^{11} - 10^{12} \text{ cm}^{-3}$  should include time-dependent ionization processes. The cooling time for a completely ionized plasma composed of electrons and ions with charge  $Z$  (due to free-free radiation alone; allowing for the recombination emission decreases this time severalfold) is  $t_c \approx 2 \times 10^{15} [s] n_e \sqrt{T/10^8} / Z$ . In real GRB, the duration of gamma-ray emission is 1-100 s and can be much smaller than the plasma cooling time.

*X-ray lines in the GRB 011211 afterglow.* XMM-Newton observations of GRB011211 afterglow [1] 11 hrs after the GRB are best fit by a thermal plasma continuum with  $T$  of several (2-4) keV and emission lines (identified with highly ionized metal species, except for iron) faded away over  $\sim 10^4$  s. In contrast to purely geometrical interpretation of these observations (which requires a very high density shell with  $n_e \sim 10^{15} \text{ cm}^{-3}$ ), our time-dependent approach identifies this time with *thermal relaxation time* of a plasma heated by passing gamma-rays up to a temperature of several keV (deposited energy  $\epsilon_0 \sim 10 \text{ keV}$  per nucleon). This time implies plasma density  $n_e \sim 10^{11} - 10^{12} \text{ cm}^{-3}$ . Then the observed

X-ray emission measure  $EM = n_e^2 V \sim 10^{69} \text{ cm}^{-3}$  means  $V \sim 10^{47} - 10^{45} \text{ cm}^3$ .

*Need for clouds.* The optical thickness w.r.t. Thompson scattering  $n\sigma_T < 1$  requires a *clumpy surroundings* with the number of clouds  $N_{cl} \sim 10^6$  of size  $l_{cl} \sim 10^{13} \text{ cm}$  and the total volume providing the required emission measure. (This is an *upper limit*: the realistic cooling function yields  $EM \sim 4 \times 10^{68} \text{ cm}^{-3}$  for normal cosmic abundance and  $EM \sim 10^{65} \text{ cm}^{-3}$  for plasma without H and He and other elements in solar ratio). The ISM with such cloudy properties is common around e.g. late AGB stars [2]. Sub-AU clouds of the density  $\sim 10^{12} \text{ cm}^{-3}$  were also involved by [3] to explain the observed short time-scale variability on GRB light curves in the external shock scenario.

*The energy deposit into surroundings.* The required energy deposit per nucleon  $\epsilon_0 \sim 10 \text{ keV}$  limits the external space where such a medium can be heated by gamma rays to the distance  $d = \sqrt{\frac{\sigma_\gamma E_\gamma}{4\pi\epsilon_0}} \sim 2 \times 10^{17} \text{ cm}$  where  $E_\gamma = 5 \times 10^{52} \text{ erg}$  is the total isotropic GRB energy,  $\sigma_\gamma \approx 0.1\sigma_T$  is the effective gamma-ray deposition cross section for heating the environment per nucleon [4]. This distance is independent of the assumed isotropy/beaming of the GRB emission. Again, this distance is strikingly similar to what is needed in the external shock scenario [3].

*GRB jet opening angle*  $\theta$  should be specified to calculate the total volume of the circumburst

\*The work is partially supported through RFBR grant 02-02-16500

matter illuminated by GRB. Assuming time delay  $t_l = 10^4$  s to be entirely due to thermal relaxation and not to geometrical retardation yields the relation  $d(1 - \cos \theta) = (ct_l)/(1 + z) \simeq 10^{14}$  cm. For small  $\theta$ ,  $d = 2 \times 10^{17}$  cm and  $z = 2.14$  we get  $\theta \sim \sqrt{2ct_l/(1+z)d} \sim 0.05$ . Such jet collimation angles  $2\theta \sim 0.1$  are common in GRB [5]. The total illuminated volume is thus  $V \sim \theta^2 d^3 \approx 3 \times 10^{49}$  cm<sup>3</sup> which implies the cloud filling factor  $f \sim 10^{45}/10^{49} \sim 10^{-4}$ . So the physically acceptable structure of clumpy ISM can actually be the source of the observed thermal X-rays from GRB 011211. For example, such a medium can be produced if several hundred late-type stars with strong winds fall within the GRB cone. Unusual in our Galaxy, this could possibly take place in star-forming galaxies at large redshifts where GRB are observed.

*Modeling the X-ray spectrum.* We use time-dependent code to compute the state of ionization and radiation of thermal plasma which include the basic elementary processes (collisional ionization, autoionization, photorecombination, dielectronic recombination, ion charge exchange) and computes free-free, free-bound, bound-bound and two-photon emission for ions of all types. The parameters include time-dependent temperature  $T$ , density  $\rho$  and chemical composition. The calculated spectral lines are shown in Fig. 1 (see [6] for more detail).

## 2. Time-dependent thermal effects in optical GRB afterglows

The GRB explosion in an inhomogeneous medium is a generic picture which is responsible for the observed variety of effects in X-ray and optical afterglow light curves (see [7] for pioneer study). We consider two possible types of surroundings: a cloudy, patchy medium and a shell-like structure around the GRB. The second case could be identified with an earlier SN explosion or intensive stellar wind of the underlying SN-type event. In both cases, a fraction of the GRB energy is deposited into the surroundings. This energy is thermalized and radiated away. If plasma of the clouds is optically thin, it rapidly cools down. The time-dependent ef-

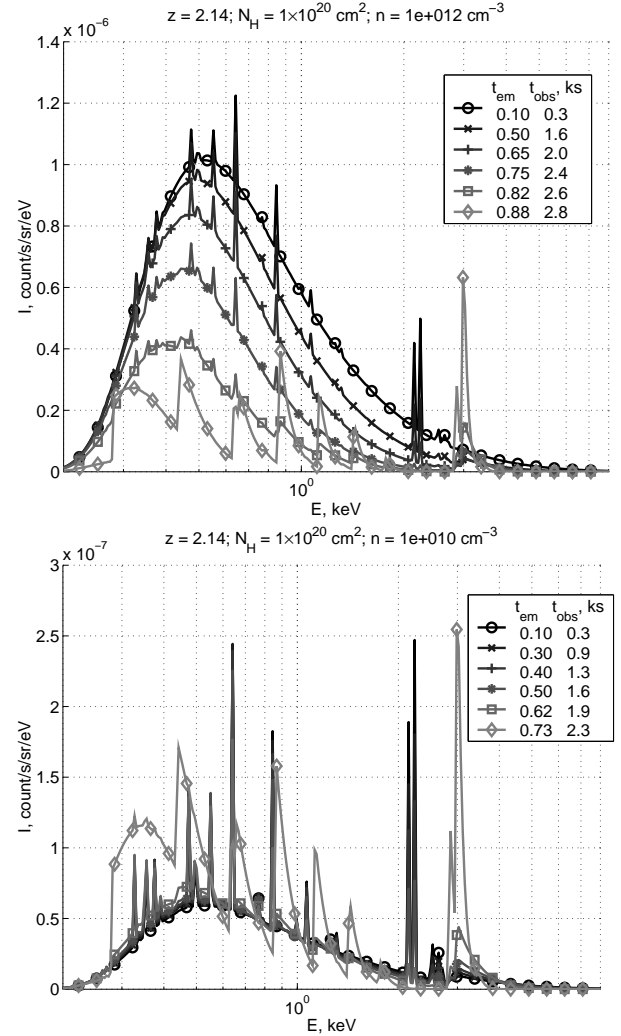


Figure 1. Time evolution of X-ray spectrum (in the observer frame at the GRB redshift  $z = 2.14$ ) for different time moments. **Upper panel:** solar composition; **Lower panel:** metal-rich plasma (without H and He).

fects from the "blue" (approaching the observer) gamma-ray beam are expected on the plasma cooling timescale  $t_c$  after the GRB, while the reverberation effects could be observed at different wavelengths later on from the "red" (receding)

jet on timescales  $t_2 \sim R(t)/c$ . Here  $R(t)$  is time-dependent distance of the photosphere (if formed) in the medium from which low-energy photons are generated. The maximum time the time-dependent effects from the "red" beam will be observed is determined by the limiting distance  $d$  and also by possible hydrodynamical effects. So the evolving "SN-like" features in the optical spectra observed in the afterglow of GRB 030329 several days – a month after the burst (also called SN 2003dh [8,9]) could be a manifestation of such effects and might have no direct relation to SN explosion.

To illustrate how the cooling plasma forms a photosphere, we present the results of LTE calculations of plasma opacities as a function of decaying temperature for a fiducial plasma density  $\rho = 10^{-14} \text{ g/cm}^3$  with normal cosmic abundance (Fig. 2). The scattering opacity is  $\kappa_T \rho \sim 3 \times 10^{-15} \text{ cm}^{-1}$  and is independent of temperature until recombination at low temperatures lowers it down to  $\sim 10^{-19} \text{ cm}^{-1}$ . These calculations indicate that up to limiting distances  $d \sim 10^{17} \text{ cm}$  (as appropriate to the case of GRB 030329), such a medium remains optically thin for scattering, but a photosphere start forming for hard photons when temperature drops below  $\sim 10^6 \text{ K}$ .

To have an idea what kind of optical events can be expected from clouds illuminated, we apply the multi-group radiation hydrocode STELLA [10] to calculate UVB-light curves (in the GRB rest-frame). We assume an energy deposit  $\Delta E$  thermalized in a homogeneous cloud ( $\rho = 10^{-14} \text{ g/cm}^3$ ) of mass  $M$  over the GRB duration time  $\Delta t$ . No equilibrium between photons and plasma is assumed. These calculations are similar to our "mini-supernova" model [11], but the difference is that here the cloud is transparent for photons so the energy is thermalized within the entire volume of the cloud. Fig. 3 shows the light curve for a large ( $R = 6 \times 10^{15} \text{ cm}$ ) cloud with a total mass of  $\sim 5M_\odot$ ,  $\Delta E \approx 6 \times 10^{49} \text{ erg}$ , and  $\delta t = 100\text{s}$ . The cloud is heated up to a temperature of  $10^4 \text{ K}$ . The optical emission from the cooling cloud continues for more than a month. For comparison, U (filled triangles), B (open squares), V (open circles) data of a typical plateau type II SN 1969L are shown. A very bright optical outburst (the

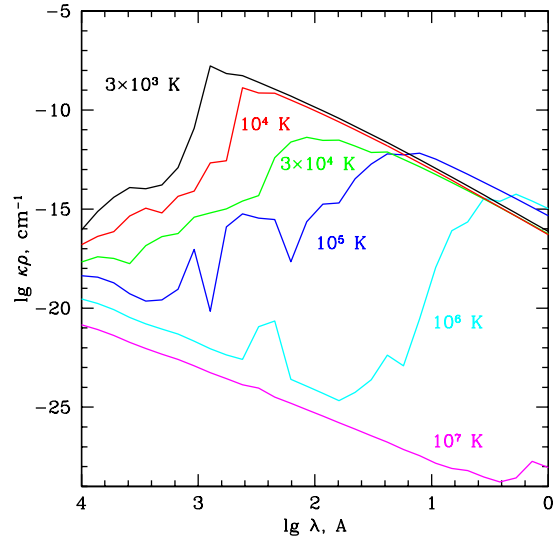


Figure 2. Scattering opacity of cooling plasma ( $\rho = 10^{-14} \text{ g/cm}^3$ ) with normal abundance.

peak absolute magnitude  $M_V \sim -21.5^m$ ) is expected shortly after the energy deposit (the light travel time correction will somewhat smear the peak on the time scale  $\sim R/c$ .) This effect can be compared with the enigmatic outburst seen in the R afterglow of GRB 030329  $\sim 1.7$  day after the GRB [12].

A different picture is obtained if we consider a smaller homogeneous cloud with  $R = 1.4 \times 10^{13} \text{ cm}$  and  $\rho = 10^{-13} \text{ g/cm}^3$  (i.e. like those required to explain non-stationary X-ray emission lines in GRB 011211). An energy deposit of  $10^{43} \text{ erg}$  into the inner  $\Delta M = 6 \times 10^{-7} M_\odot$  over  $\Delta t = 10 \text{ s}$  heats up the cloud to  $T \sim 40000 \text{ K}$ . This yields (Fig. 4)  $M_{opt} \sim -5^m \dots -7^m$ . A collection ( $10^5 - 10^6$ ) of such clouds (patchy presupernova wind?) at  $d \sim 10^{17} \text{ cm}$  would naturally produce a reverberating optical bump with  $M_{op} \sim -17^m \dots -19^m$  on the optical light curve of the canonical power-law GRB afterglow several weeks after the GRB. It is still to be explored if such clouds can mimic spectrum of a SN Ic event spectroscopically identified in GRB 030329 [8,9].

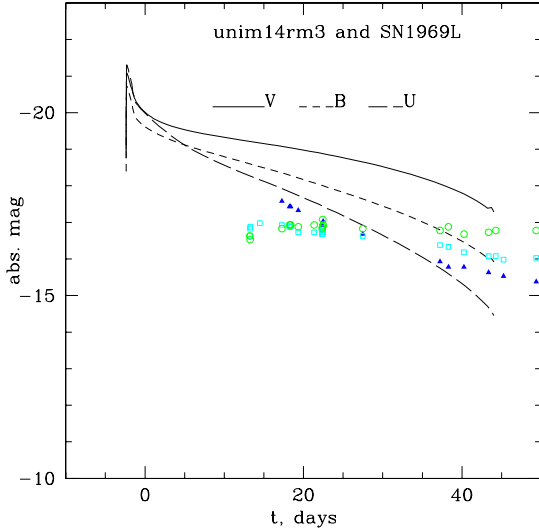


Figure 3. The "mini-SN" effect from a large homogeneous cloud with  $R = 6 \times 10^{15}$  cm after energy deposit  $\Delta E \approx 6 \times 10^{49}$  erg. SN 1969L is shown for comparison.

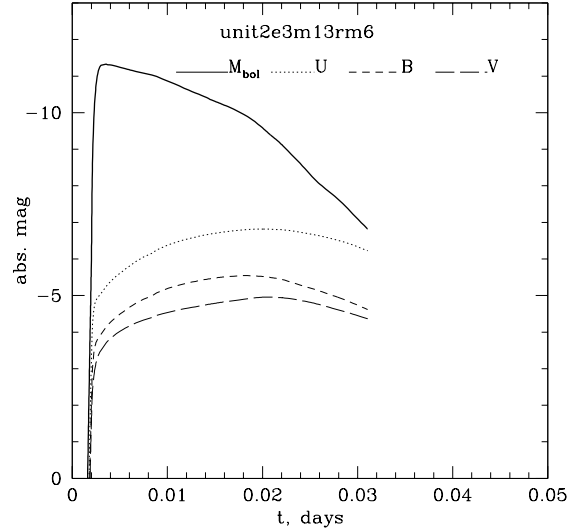


Figure 4. Thermal relaxation of a small homogeneous cloud with  $R = 1.4 \times 10^{13}$  cm after thermalizing  $\Delta E = 10^{43}$  erg inside the inner  $\Delta M = 6 \times 10^{-7} M_{\odot}$ .

### 3. Conclusions

Time-dependent thermal plasma effects from GRB surroundings should manifest in X-ray and lower energy afterglows of a GRB twofold:

(1) Shortly after GRB (on the plasma cooling time scale determined by density, chemical composition and the energy deposited over the GRB emission time) thermal effects may be produced by plasma heated up by the "blue" GRB jet. The fading X-ray emission lines in GRB 011211 may provide an example.

(2) At later times, variable thermal optical features can be observed superimposed on the underlying non-thermal afterglow continuum due to the contribution from cooling clouds/shells heated by the receding ("red") GRB jet on timescales limited by the most remote clouds  $d$ . Optical afterglows of GRB 021004 and GRB 030329 deviating from pure power-law can provide the example. The effective photosphere moving across the

heated region can mimic the SN-like effects observed in some GRB.

### REFERENCES

1. J.N. Reeves et al., Nature 416 (2002) 512.
2. I. Bains et al., MNRAS 342 (2003) 8.
3. C.D. Dermer and K.E. Mitman, ApJ 513 (1999) L5.
4. K. Ambwani and P. Sutherland, ApJ 325 (1988) 820.
5. D.A. Frail et al., ApJ 562 (2001) L58.
6. D.I. Kosenko et al., Astron. Letters 29 (2003) 205.
7. G.S. Bisnovatyj-Kogan and A.N. Timokhin, Astron. Rep. 41 (1997) 423.
8. K.Z. Stanek et al., ApJ 591 (2003) L17.
9. J. Hjorth et al., Nature 423 (2003) 847.
10. S.I. Blinnikov et al., ApJ 496 (1998) 454.
11. S.I. Blinnikov and K.A. Postnov, MNRAS 293 (1998) L29.

12. T. Matheson et al., astro-ph/0307435.